# Time-dependent breakdown of fiber networks: Uncertainty of lifetime

Amanda Mattsson* and Tetsu Uesaka†
*Department of Chemical Engineering, Mid Sweden University, Sundsvall, Sweden 85170*
(Received 30 January 2017; published 30 May 2017)

Materials often fail when subjected to stresses over a prolonged period. The time to failure, also called the lifetime, is known to exhibit large variability of many materials, particularly brittle and quasibrittle materials. For example, a coefficient of variation reaches 100% or even more. Its distribution shape is highly skewed toward zero lifetime, implying a large number of premature failures. This behavior contrasts with that of normal strength, which shows a variation of only 4%–10% and a nearly bell-shaped distribution. The fundamental cause of this large and unique variability of lifetime is not well understood because of the complex interplay between stochastic processes taking place on the molecular level and the hierarchical and disordered structure of the material. We have constructed fiber network models, both regular and random, as a paradigm for general material structures. With such networks, we have performed Monte Carlo simulations of creep failure to establish explicit relationships among fiber characteristics, network structures, system size, and lifetime distribution. We found that fiber characteristics have large, sometimes dominating, influences on the lifetime variability of a network. Among the factors investigated, geometrical disorders of the network were found to be essential to explain the large variability and highly skewed shape of the lifetime distribution. With increasing network size, the distribution asymptotically approaches a double-exponential form. The implication of this result is that, so-called "infant mortality," which is often predicted by the Weibull approximation of the lifetime distribution, may not exist for a large system.

DOI: 10.1103/PhysRevE.95.053005

## I. INTRODUCTION

Time-dependent failure typically appears in creep and fatigue, in which the material is subjected to relatively low levels of loading over time. It is normally characterized by the time to failure, i.e., the lifetime. However, a common measure of "strength," herein called the static strength, is determined by monotonically increasing the load to the point of final failure. The latter is intended to predict the former, but practical experience shows that stronger materials do not necessarily exhibit longer lifetimes. The most important difference between lifetime and static strength is lifetime's enormous variability: static strength typically varies with a coefficient of variation (COV) of only 4%–10%, whereas lifetime can easily vary with a COV of 100% or even 200% under nominally constant mechanical and environmental conditions (e.g., [1–8]).

A natural question is why lifetime variations are so large as compared with those of static strength, and/or what controls lifetime variations. Part of the answer for this question has been given by a seminal work by Coleman ([9–11]) and the recent work by Christensen (e.g., [12,13]). Coleman derived an expression for the cumulative distribution function of lifetime for an arbitrary loading history based on the three postulates: (1) weakest-link scaling (WLS), (2) an algebraic form of the probabilistic failure criterion, and (3) damage evolution rules (exponential or power-law forms). Christensen considered the time-dependent extension of a single crack, and obtained the lifetime distribution for creep by assuming that (1) the crack growth rate is the power-law function of stress, (2) the crack unsteadily grows at a critical stress intensity, and (3) the strength measured in a far field follows Weibull distribution. They arrived at the following relationship between static strength variability and creep lifetime variability:

$$\beta_{\text{strength}} = (\rho + i)\beta_{\text{creep}}, \tag{1}$$

where $\beta$ refers to Weibull exponent for either static strength or creep lifetime, $\rho$ is a stress-related exponent for damage (or crack) growth, and $i = 1$ for Coleman's model, and $i = 0$ for Christensen's model. (For brittle and quasibrittle cases, as $\rho \gg 1$, both approaches essentially give the same result.) According to this relation, the seemingly small variability (i.e., high Weibull exponent) of static strength is due to the high stress sensitivity of damage growth (high $\rho$) for brittle or quasibrittle materials. Although the approaches taken by Coleman and Christensen are phenomenological, they have provided a powerful tool for organizing hopelessly-scattered creep lifetime data. In addition, many of the postulates included in their formulations are also touching upon some of the key topics of statistical physics: disorders and damage growth, size scaling, the validity of Weibull distribution, and the onset of avalanche failure.

The first basic question is why failure parameters exhibit statistical distributions. In the case of quasistatic statistical failure (QSF), where the literature abounds (an extensive review is found in, e.g., [14]), it is defects and/or disorders that cause statistical failure. Therefore, it is almost customary in the literature to start with preexisting defects, such as burned fuses and broken bonds, and threshold strength distributions. Without these, static strength is, obviously, deterministic. On the other hand, when we consider time-dependent statistical failure (TSF) [1,15,16], we do not necessarily start from the defects and threshold strength distributions, but from an underlying stochastic process, i.e., the continual breaking and reformation of "bonds" due to thermal fluctuations [11]. That is, there is always a nonzero probability of failure

*amanda.mattsson@miun.se
†tetsu.uesaka@miun.se

 

per unit time when stress is applied, no matter how small it is. Therefore, without predefining defects and threshold strength distributions, a failure parameter, such as lifetime, shows statistical variations. Defects are actually a natural consequence of damage growth, i.e., the interplay between this underlying stochastic process and hierarchical and disordered structures that affect stress distributions [15,17].

The size dependence of distribution functions, hereby called "size scaling," is one of the most fundamental and controversial subjects of strength theories. (Extensive reviews of different scaling laws are given in the literature, e.g., [18–20].) The most frequently used scaling law, WLS, is defined by

$$1 - F_N(x) = [1 - W(x)]^N, \tag{2}$$

where $F_N$ is the cumulative distribution function (CDF) of $x$ for the system size $N$, and $W(x)$ is a function independent of the system size, often called the characteristic distribution function. The WLS hypothesis is most frequently used for brittle and quasibrittle systems, because it presumes that a dominant damage cluster (or crack) just before failure is confined in a small volume (representative volume element) as compared with the system size. However, it is difficult to test this simple hypothesis experimentally (e.g., [21]), because of the lack of appropriate equipment to allow testing varying-size specimens. Therefore, researchers have taken either numerical approaches or, if possible, analytical approaches, using simple lattice and network models, such as random fuse models (RFMs) and fiber-bundle models (FBMs). For static strength, fiber-bundle models have been extensively used to investigate size scaling both analytically and numerically (e.g., [1,4,10,16,17,22–28]). In these FBM studies, the load released by a failed fiber is shared only in the neighboring fibers (local-load sharing or extended load sharing) to mimic brittle and quasibrittle failure. [For those cases of more ductile and soft materials, global-load sharing in FBMs is applicable. Extensive reviews are available (e.g., [29,30]).] The results from Monte Carlo simulations showed that "WLS-like" scaling does appear when the system size grows, but the emergence of WLS-like behavior is rather slow. The analytical studies (e.g., [31]) also supported the observations from numerical studies that WLS certainly appears asymptotically as the system size grows. Generally speaking, Monte Carlo simulations did suggest scaling trends, but it is still difficult to confirm the exact form of scaling, even with the simple lattice models and today's computational capacity [28].

The Weibull distribution has been observed for both static strength and lifetime for many years in the engineering literature (a good overview in [32]). The ubiquitous nature of the Weibull distribution is often attributed to the fact that it is one of the three limiting distributions of extreme-value statistics (i.e., Weibull, Gumbell, and Fréchet distributions) [33]. The most obvious case is a one-dimensional material, such as fiber, which shows WLS and thus Weibull distribution for samples of a sufficiently long length [9]. However, it has been also known that non-Weibull distributions are quite commonly seen in fiber-bundle systems. Particularly, numerical simulations of the fiber-bundle failure (static strength), with the local-load sharing rule, consistently showed slightly heavier, upper and lower tails when strength distributions are plotted in the Weibull form (e.g., [16,17,26]). Although, in experiments, it is difficult to detect this non-Weibull behavior in a statistically significant manner, the deviation is sometimes noticeable (e.g., [21]). Duxbury and co-workers started, in the late 1980s, analytical and numerical studies of the static strength distributions, initially with random fuse model and later a-chain-of-fiber bundles model, and have derived an alternative distribution, a double-exponential form [31,34–36]. (We tentatively call it DLB-type distribution by following the recent literature [37,38].) Although this distribution form does not look at any of the three extreme-value distributions, they have demonstrated [31] that it asymptotically approaches, although extremely slowly, Gumbel distribution. DLB-type distribution well represents the heavier upper and lower tails of the distributions which are numerically observed. The recent scaling studies, together with numerical confirmation with the random fuse model, have provided further support to this new distribution form [37,38]. An interesting question is, then, whether this distribution form is extended to TSF. As argued by Curtin and Duxbury and co-workers [35,39], if the tail of the (preexisting) damage cluster size distribution is approximated by an algebraic form, the resulted static strength distribution is the Weibull distribution, whereas if it is an exponential form, it leads to the double-exponential form. Since, in the case of TSF, the damage clusters naturally evolve, instead of being predetermined either in the algebraic or exponential forms, it is interesting to see the consequence of such evolution of damages to the lifetime distribution.

In our earlier study [40], we performed Monte Carlo simulations of creep failure for a two-dimensional (2D) central-force, triangular-lattice fiber network. Such system may be regarded as a paradigm of a broader class of networks, e.g., amorphous polymers, biological tissues, industrial materials (paper and nonwoven), and even electrical power grids. We found that Coleman's postulates hold even in this 2D system, except for size scaling, and the system behavior is characterized by three parameters: the characteristic strength (short-term strength), a brittleness parameter, and Weibull shape parameter (related to the creep lifetime distribution). Based on this formulation, we started investigating the effect of disorders on lifetime variability. For the type of disorders, we chose the characteristic strength of fiber (corresponding to threshold strength for QSF) and elastic stiffness of fiber by drawing the values from uniform distributions of varying width. For both cases we observed that

$$\beta_s \geqslant \beta_f, \tag{3}$$

where $\beta_s$ and $\beta_f$ are Weibull exponents for the system and the fiber, respectively. The system's Weibull exponent was always higher than that of the fiber, even when the disorder of either threshold strength or stiffness is very strong. This means that, if the elementary stochastic process is memoryless (Markov process, $\beta_f = 1$), then $\beta_s \geqslant 1$. This result raises an interesting question, why experimental data, as mentioned earlier, almost regularly show the values of Weibull exponent less than 1.

Based on our previous study, we here examine how these three material parameters are related to the system size, fiber characteristics, and network structures. For the system size, we examine scaling laws, without edge effects, and derive the characteristic distribution function for the lifetime. We show that the lifetime distribution for a large system takes a

double-exponential form, instead of the Weibull form. We demonstrate that fiber characteristics, particularly fiber brittleness, have a direct and sometimes dominating influence on a network's failure. Lastly, we examine both regular and random network structures and show that the geometrical disorder of a network is a critical factor contributing to the large lifetime uncertainty.

## II. CHARACTERIZATION OF TIME-DEPENDENT STATISTICAL FAILURE

Lifetime distribution depends, not only on load applied at the time of failure, but more generally on loading histories. This situation is different from the case of QSF. In this section we find a possible form of the relationship between the loading history and the lifetime distribution for a fiber network. This is for defining characteristic parameters of TSF that can be extracted from numerical experiments. A fiber network here is defined as a system of connected fibers at nodes, but the network geometry is not necessarily specified. We assume that the time-dependent failure of a fiber is characterized by the following CDF of lifetime, as given by Coleman's TSF model [9]:

$$F_i(t) = 1 - \exp\left\{-A\left[\int_{s=0}^{t} f_i(s)^{\rho} ds\right]^{\beta}\right\}, \tag{4}$$

where $F_i(t)$ is the probability that the lifetime of the $i$th fiber is less than $t$, $f_i(s)$ is a loading history applied to the $i$th fiber, and $A$, $\rho$, and $\beta$ are material constants. When considering the CDF of a fiber *network*, this equation restricts the possible forms of the CDF. For example, Eq. (4) can be rewritten by changing the variable in the time integration:

$$F_i(t) = 1 - \exp\left\{-At^{\beta}\left[\int_{\hat{t}=0}^{1} f_i(\hat{t})^{\rho} d\hat{t}\right]^{\beta}\right\}, \tag{5}$$

where $t^{\beta}$ is a *global* variable, i.e., it is not dependent on the specific fiber "$i$" or on a specific network structure, but appears in the final CDF of the fiber network as is. Therefore, if the final CDF has an algebraic dependence on time in the form of $t^{\alpha}$, then its exponent $\alpha$ must be proportional to $\beta$. Another restriction concerns the dependence on $\rho$. Suppose the network receives a time-varying loading history $S(t)$; then, the corresponding load applied to the fiber "$i$" may be expressed as $f_i(t) = S(t)K_i(t)$, with $K_i(t)$ as the stress concentration factor. Inserting this expression into Eq. (4), we obtain

$$\begin{aligned} F_i(t) &= 1 - \exp\left\{-A\left[\int_{s=0}^{t} [S(s)K_i(s)]^{\rho} ds\right]^{\beta}\right\} \\ &= 1 - \exp\left\{-A\left[\int_{z=0}^{\tau} [K_i(z)]^{\rho} dz\right]^{\beta}\right\}, \end{aligned} \tag{6}$$

where $dz = S(s)^{\rho} ds$, $\tau \equiv \int_{s=0}^{t} S(s)^{\rho} ds$, and $\tau$ is assumed to be a single-valued, monotonically increasing function, with $S(\cdot)$ as a positive continuous function. Equation (6) shows that the dependence on the external load is included in the transformed time variable $\tau$; this time variable is again a global variable, which is elevated to the network level across different structure scales (if any). This result implies that the effect of a load applied to the network should appear in the form of $S^{\rho}$ in the network CDF. Note, however, that the relation $f_i(t) = S(t)K_i(t)$ requires that the system should be elastic (unique) and undergo small deformation (i.e., geometrically linear). Based on these criteria, we seek a possible form of the CDF for a fiber network. First, we recast the CDF of a single fiber in a nondimensional form:

$$F_i(\tilde{t}) = 1 - \exp\left\{-\left[\int_{s=0}^{\tilde{t}} \left(\frac{f_i(s)}{T_c}\right)^{\rho_f} ds\right]^{\beta_f}\right\}, \tag{7}$$

where $T_c$ is the characteristic strength of the fiber [$T_c = (t_0/A)^{1/\rho_f}$] and $\tilde{t}$ represents nondimensional time $t/t_0$, with $t_0$ being an appropriate time constant. (We subsequently drop the tilde with the understanding that time is nondimensionalized.) We also add a subscript "$f$" to denote the material constants for the fiber. Then, one of the possible forms of the fiber network CDF, $F_s(t)$, that satisfies the previous two conditions, is actually the same form as that for a single fiber:

$$F_s(t) = 1 - \exp\left\{-\left[\int_{s=0}^{t} \left(\frac{S(s)}{S_c}\right)^{\rho_s} ds\right]^{\beta_s}\right\}, \tag{8}$$

where $S_c$, $\rho_s$, and $\beta_s$ are the corresponding parameters for the fiber network. The parameter $S_c$ is the characteristic strength of the network, the creep load at which the material fails within a unit time with a probability of $1 - 1/e$ ($= 0.6321$), i.e., a measure of short-term strength. The parameter $\beta_s$ is a Weibull shape parameter of creep lifetime distribution, i.e., long-term reliability. From its definition in the damage evolution law (damage evolution rate $\propto f_i^{\rho}$) [9], $\rho_s$ is regarded as a measure of brittleness of the network. An advantage of this form is that the parameters $\beta_s$ and $\rho_s$ can be measured in creep tests independent of the above equation, and such data are found in the experimental literature. In other words, by determining these parameters by modeling, we can directly connect the numerical work to experimental data available in the literature. The form of Eq. (8) was originally suggested by Curtin and Scher [15], and our earlier result of load scaling of the creep lifetime distribution supports their claim [40]. An important difference between the single-fiber CDF and the network CDF is that these material parameters are generally a function of the system size, whereas for the single-fiber CDF, $\rho_f$ and $\beta_f$ are independent of the size of the fiber.

From the previous two constraints, we derive the following relationships between the material constants for the fiber and network:

$$\rho_s = \rho_f \quad \text{and} \quad \beta_s = a\beta_f, \tag{9}$$

where $a$ is a material constant related to the network.

## III. SPRING NETWORK FOR TIME-DEPENDENT, STATISTICAL FAILURE

### A. Model geometry and boundary conditions

The spring network we use is a central-force, triangular-lattice network (Fig. 1). This model has a long history in the literature in the context of statistical failure (e.g., [15,41,42]). The advantage of this model is that, even though the geometry is highly simplified, the model retains the essential network

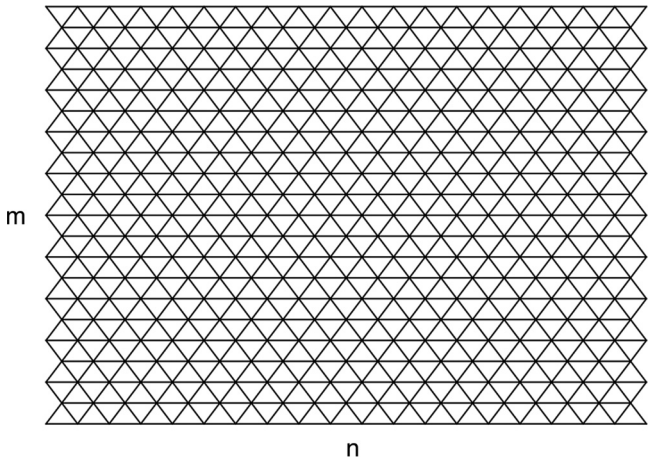


FIG. 1. Schematic of the default central-force, triangular lattice used in the simulations. The load is applied in the vertical direction.

mechanics (long-range correlation) and rich statistical mechanics, equivalent to the full-scale fiber network model we investigated earlier [43]. Unlike FBM, this model does not require defining special load-sharing rules, such as global load sharing and local load sharing. Load sharing is determined by force equilibrium. Another important point to note is that the coordination number of this system is 6, larger than 4, i.e., the isostaticity point in 2D, at which the degree of freedom and the number of constraints are equal [44–47]. Therefore, the initial structure of this network is rigid, unlike some of the percolated network models (e.g., [48]). With this model, disorders can be introduced into the properties of the element (fiber), such as stiffness and characteristic strength of fiber, and also into the network geometry, as will be described later. In this study we did not introduce so-called "defects" (missing elements or burned fuses in RFMs) into the network. This is because this type of disorder simultaneously changes several important aspects of the network properties, such as overall rigidity, the threshold strength distribution (i.e., binary distribution), and local network topology, and thus it is difficult to interpret results afterward.

Constant tensile force is applied at the top boundary to simulate creep. The traction-free boundary condition is employed at the sides. In our earlier study, we found significant edge effects of the traction-free boundaries on size scaling [40]. However, periodic boundary conditions are not used in this study to avoid introducing artificial length scales for the failure phenomena. Instead, the two upper rows and the two side edges are prevented from failing to avoid instabilities induced by large rotation of the failed elements and to eliminate typical edge effects. Each element has the same elastic modulus and the same length and diameter. In this study we did not introduce viscoelastic constitutive laws, such as Kelvin or Maxwell models, for the fiber (e.g., [49]), but focus on the creep induced by damage evolution. The size of the network is described by $m$ (the number of stacks) and $n$ (the number of horizontal fibers), as shown in Fig. 1.

### B. Fiber failure model

The fiber is assumed to break according to the time-dependent failure model, Eq. (7). In this paper we set $\beta_f = 1$. The significance of $\beta_f = 1$ is that the probability of failure per unit time is given by

$$h(t) = \frac{F_f'(t)}{1 - F_f(t)} = \left(\frac{T(t)}{T_c}\right)^{\rho_f}. \tag{10}$$

That is, it is determined only by the force at the current time and not the force in the past (memoryless, or Markov process). We choose the element failure rate as memoryless to investigate the origins of the system's memory ($\beta_s$).

The simulations start with applying a dead load, and the forces acting on individual fibers are calculated. Based on these forces, random numbers are generated according to Eq. (7), and the lifetime values for individual fibers are calculated. The fiber with the shortest lifetime is chosen to break, and the modulus for this fiber is set to zero (or a small number). Then, the forces in each fiber are recalculated for the new state of mechanical equilibrium. Lifetime values of survived fibers are updated using the following formula:

$$t_{B2} - t_1 = \left(\frac{T(0)}{T(t_1)}\right)^{\rho} (t_{B1} - t_1), \tag{11}$$

where $t_1$ is the time of the first fiber failure in the *system* and $t_{B1}$ and $t_{B2}$ are the first and the second estimates of lifetime of a surviving fiber, respectively. $T(0)$ and $T(t_1)$ are the forces of the surviving fiber before and after the first fiber failure, respectively. The minimum of the updated lifetimes of all surviving fibers is then identified; this determines the second fiber failure. This process continues until avalanche failure occurs. This algorithm more faithfully reproduces fiber breaking processes than the earlier method for triangular lattice models (e.g., [15,41,42]) and is in the same spirit of those used for fiber bundle models (e.g., [50]). The avalanche failure of the network is defined by the following two conditions: the ratio of the current rate to the initial rate of creep exceeds a certain value $r$, and this high creep rate ($r$) is repeated for a certain number of consecutive time steps $n$. Within the parameter space tested, we have found that $r = 100$ and $n = 5$ can consistently detect the initiation of avalanche failure.

The stiffness equation of the system was solved using a truss analysis code [51] together with a MATLAB sparse matrix library to enable larger-scale simulations. The default set values used for the fibers (truss elements) in the model are controlled in order to limit the overall deformation within a small strain (geometrically linear) range. Denoting the characteristic strength as $T_c$, elastic modulus as $E_f$, cross-sectional area as $A$, and the applied load at each node as $S_0$, we used $T_c/S_0 = 10/3$ and $E_f A/S_0 = 500/3$ as default values to avoid large deformation. The default value of $\rho$ was 10, and was later varied from 5 to 200 to accommodate quasibrittle to brittle failure modes.

In our previous paper [40], we investigated effects of random distributions of characteristic strength of fiber ($T_c$) and fiber stiffness ($A$) by drawing the numbers from uniform distributions. Here we focus on structural disorders by comparing the regular structure and randomly distorted structures.

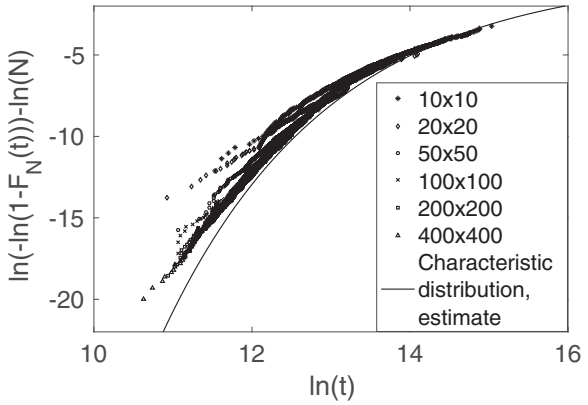


FIG. 2. Lifetime distributions for different system sizes plotted in Weibull format. $N$: The total number of fibers. The broken line is an estimate of the characteristic distribution function. The total number of repetitions is 1000 for each system size and each load.

### C. Determination of material parameters

The material parameters are determined by solving Eq. (8) for creep [$S(s) = S_0 =$ is constant for $s \geqslant 0$]:

$$F_s(t) = 1 - \exp\left\{-\left(\frac{S_0}{S_c}\right)^{\rho_s \beta_s} t^{\beta_s}\right\}, \tag{12}$$

and by taking the Weibull transform of the above equation:

$$\ln\{-\ln[1 - F_s(t)]\} = \rho_s \beta_s \ln S_0 - \rho_s \beta_s \ln S_c + \beta_s \ln t. \tag{13}$$

From this Weibull transform, we have determined the material parameters on the right-hand side using a nonlinear regression, instead of the maximum-likelihood method (MLM), because MLM has been found to be not always stable for a wide range of the parameter space.

## IV. RESULTS

### A. Lifetime distribution and size effect

We begin our investigation with a 2D fiber network with an ordered structure (Fig. 1). Lifetime distributions of creep failure are shown in Fig. 2 for different system sizes, where $m$ and $n$ denote length and width, respectively (Fig. 1). The data are plotted in a Weibull format: if the distributions follow the Weibull distribution, the plots appear as straight lines, and if WLS appears, then all data points collapse onto one single curve (or line). First, individual plots are approximately linear, i.e., they follow the approximate Weibull distribution, confirming a number of experimental observations in the literature. Second, as the system size increases, each distribution has a tendency to move toward a converged curve, i.e., WLS seems to emerge with increasing system size, although this asymptotic behavior is rather slow, as expected [28].

Using the data of lifetime distributions at different loads at a given system size, we can determine three material parameters: (1) the characteristic strength, $S_c$, (2) the brittleness parameter, $\rho_s$, and (3) the Weibull shape parameter (long-term reliability parameter), $\beta_s$, as described earlier.

Figure 3 shows the size dependence of each parameter. In this graph, typical error bars for each data point are of the same size as the plotting symbols. (For example, the standard error of $\beta_s$ was $5.8526 \times 10^{-3}$ for an estimate of 2.5586; thus the relative error was 0.2%. The relative errors for the two other parameters, $S_c/T_c$ and $\rho_s$, were even lower.) The parameter $S_c$ decreases very slowly with the size $N$, as shown by its logarithmic dependence. The parameter $\rho_s$ maintains the value corresponding to the fiber (=10) and is independent of the system size. In other words, the load dependence is preserved when moving up in the structural hierarchy from fiber to network. The parameter $\beta_s$ continues to increase with increasing size $N$, but relatively slowly, with a logarithmic dependence. Interestingly, this logarithmic dependence was predicted by an analytical model of damage evolution by Curtin and Scher [15]. The increase of the Weibull shape parameter with the system size has previously been reported experimentally (in terms of the static strength of concrete [19] and paper materials [21]) and also numerically by fiber-bundle models with local load sharing.

These relations are summarized as

$$\ln\left(\frac{S_c}{T_c}\right) = a_s \ln[\ln(N)] + b_s, \tag{14}$$

$$\rho_s = 9.9942 \approx \rho_f = 10, \qquad \text{and} \tag{15}$$

$$\beta_s = a_b \ln(N) + b_b, \tag{16}$$

where $a_s = -0.2116$, $b_s = 0.5261$, $a_b = 0.4536$, and $b_b = -0.1205$. Clearly, these size-scaling relations are different

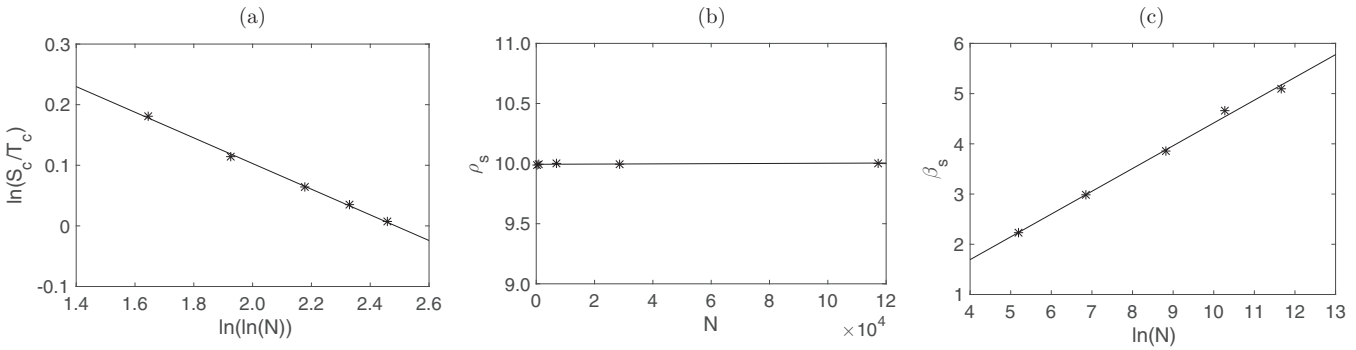


FIG. 3. Effect of the size of the system (N: the total number of fibers) on (a) nondimensionalized characteristic strength, $S_c/T_c$, (b) brittleness parameter, $\rho_s$, and (c) Weibull shape parameter, $\beta_s$.

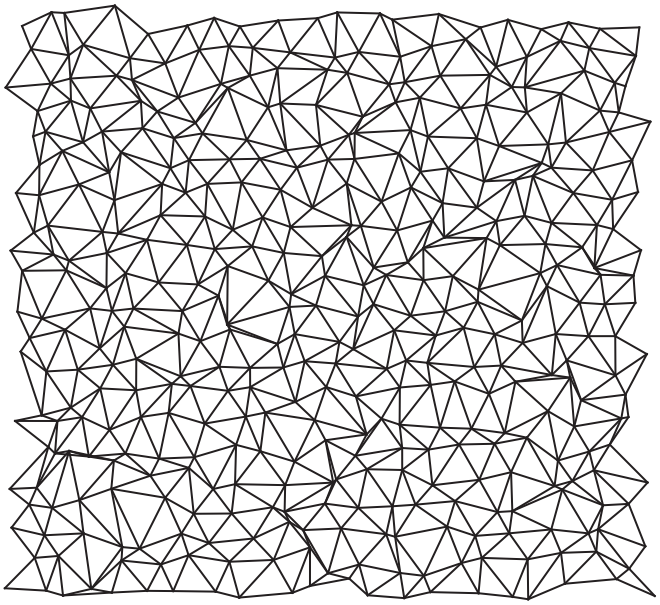

FIG. 4. Schematic of a distorted structure of the triangular lattice.

from those predicted from the traditional Weibull statistics: $\ln(S_c)$ is linearly related to $\ln(N)$, instead of $\ln[\ln(N)]$, and $\beta_s$ is constant over scale.

Based on these equations, we estimate a distribution function that would emerge if WLS arises, i.e., a characteristic distribution function [16]. We first denote the characteristic distribution function as $W(t)$. As the emergence of WLS is rather slow, the best estimate of $W(t)$ may be obtained by using the conjecture employed by Phoenix and Tierney [26] and Newman and Phoenix [16]. That is, each Weibull-transformed curve in Fig. 2 is assumed to form a tangent to $[1 - W(t)]$. This conjecture leads to the following relation:

$$[1 - F_N(t)]^{(1/N)} = [1 - F_{N+1}(t)]^{[1/(N+1)]}. \tag{17}$$

Solving the above equation for $N$ with Eqs. (14)–(16) and inserting it into Eq. (7), we obtain an expression for $W(t)$:

$$1 - W(t) \approx \exp\{-\exp[-pt^{-1/q} + d]\}, \tag{18}$$

or, for a small value of $\exp\{-pt^{-1/q} + d\}$,

$$W(t) \approx \exp\{-pt^{-1/q} + d\}, \tag{19}$$

where $p = 3.72 \times 10^3$, $q = 2.12$, and $d = -0.0099$. The estimated characteristic distribution is plotted in Fig. 2. Equation (19) gives a double-exponential form of the lifetime distribution:

$$F_N(t) = 1 - \exp\{-rN\exp[-pt^{-1/q}]\}, \tag{20}$$

where $r = \exp\{d\} \cong 1$. Very interestingly, this form was the DLB-type distribution for static strength obtained by Duxbury and co-workers for random fuse model [34] and fiber-bundle models [31,35,36]. In these studies, the distribution was obtained by introducing various types of predefined disorders, such as percolated disorders, threshold strength distributions, and crack length distributions. In this study, however, we let damage naturally grow over time according to the underlying stochastic process [Eq. (7)] without assuming any initial disorders. In our previous study [40] we observed the same form of the distribution function even if there exists the natural edge effect in the traction-free boundaries.

### B. Effects of disordered structure

In this section, we tackle the question of how disordered structures influence the material parameters $S_c$, $\rho_s$, and $\beta_s$. We have chosen $100 \times 100$ as the size of the network, at which the lifetime distributions start approaching the characteristic distribution function. The position of each node is distorted by Gaussian random variables with zero mean and varying standard deviation (SD) (Fig. 4). The coordination number (=6) is kept constant so that the initial structure is rigid in the sense that it is above the isostaticity point (=4). The brittleness parameter of the fiber is varied on two levels: $\rho_f = 10$ (quasibrittle) and $\rho_f = 50$ (brittle).

Figure 5 shows the results for the material parameters. First, with increasing SD, the characteristic strength, $S_c$, decreased almost linearly. Particularly, for $\rho_f = 50$, $S_c$ decreased more rapidly than for $\rho_f = 10$. Apparently, for a more brittle system, (characteristic) strength is more sensitive to the structural disorder. The parameter $\rho_s$ remained constant and kept its corresponding values for the fiber (10 and 50). In other words, the brittleness parameter $\rho_s$ is entirely controlled by that of the fiber and not by the structural disorder. The Weibull shape parameter, $\beta_s$, decreased with the degree of distortion, SD. More brittle fibers ($\rho_f = 50$) consistently showed lower $\beta_s$ values. Interestingly, $\beta_s$ went below unity, which is the value of $\beta_f$ (i.e., the shape parameter for the fiber). Note that

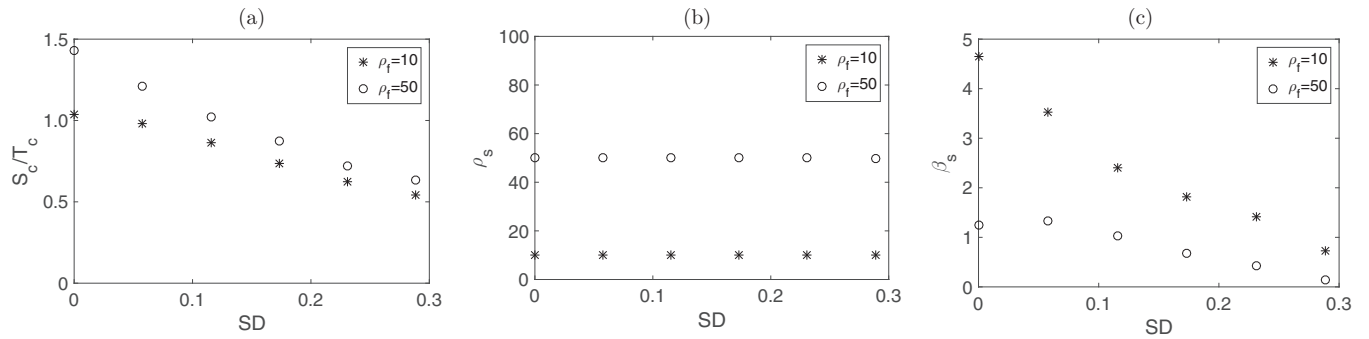


FIG. 5. Effect of the distortion of the structure for two cases of the fiber property, $\rho_f$, $\rho_f = 10$ and $\rho_f = 50$, on (a) nondimensionalized characteristic strength, $S_c/T_c$, (b) brittleness parameter, $\rho_s$, and (c) Weibull shape parameter, $\beta_s$. SD: standard deviation.

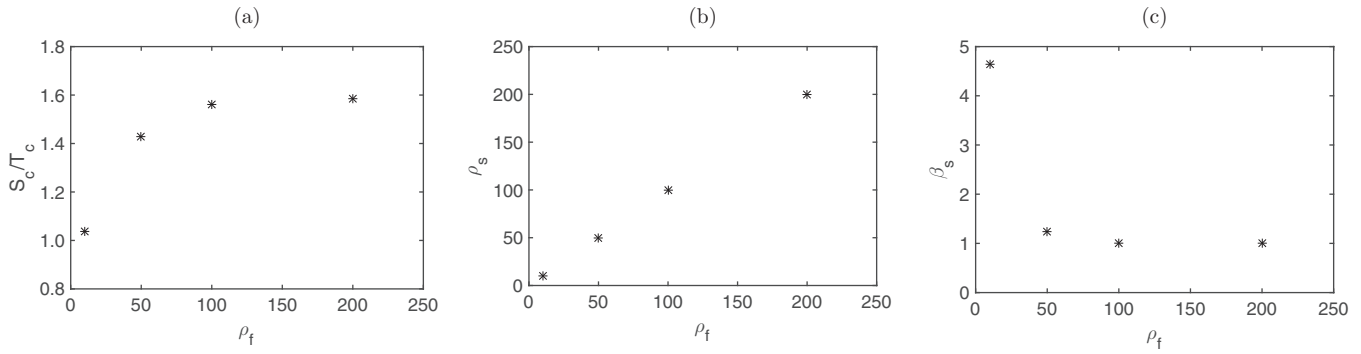


FIG. 6. Effect of the fiber property, $\rho_f$, on (a) nondimensionalized characteristic strength, $S_c/T_c$, (b) brittleness parameter, $\rho_s$, and (c) Weibull shape parameter, $\beta_s$.

all fiber-bundle models proposed for time-dependent failure (e.g., [16,26,52]) have so far showed $\beta_s \geqslant \beta_f$. Such result is reasonable because the load-sharing structure of a FBM tends to suppress the variability of lifetime at the network level, as seen in the analytical solution for the equal-load-sharing case (e.g., [16]). Even in our previous case of the two-dimensional, triangular lattice network [40], we still observed that $\beta_s \geqslant \beta_f$, for the large variations in the fiber stiffness and fiber characteristic strength [40]. Experimental data, however, commonly show less-than-unity values of $\beta_s$ [1–7]. Typically, the values for fibers and filaments (e.g., glass fiber, carbon fiber, and graphite fiber) tend to be much less than unity, whereas those for fiber composites (load-sharing structures) and fiber networks tend to be higher, being sometimes more than unity. The result obtained here has, therefore, an important implication regarding the long-term material uncertainty, as we will discuss in later sections.

### C. Effects of fiber brittleness parameter, $\rho_f$

The brittleness parameter of the fiber $\rho_f$ also affects the system's properties, i.e., $S_c$, $\rho_s$, and $\beta_s$ (Fig. 6). The parameter is varied from a typical quasibrittle range (e.g., $\rho_f = 10$) to a super-brittle range (e.g., $\rho_f = 200$, corresponding to graphite fiber [5]). With increasing $\rho_f$, the characteristic strength, $S_c$, sharply increases and reaches a plateau in the high brittleness range. The parameter $\rho_s$ is equal to the fiber $\rho_f$, as predicted earlier. The parameter $\beta_s$ decreases sharply with increasing $\rho_f$ and plateaus in the high brittleness range. These results are qualitatively consistent with experimental observations in the literature: higher brittleness of the component fiber ($\rho_f$) is often associated with higher (short-term) strength ($S_c$) but poor long-term reliability ($\beta_s$) (or increased uncertainty, e.g., [5,6]).

### D. Critical damage cluster

It is known that for a homogeneous elastic continuum, there is a critical crack length at which unstable crack growth initiates. Linear-elastic fracture mechanics theory asserts that the critical crack $a_c$ satisfies $\sigma_\infty \sqrt{a_c} = C$ at a given far-field stress $\sigma_\infty$. The constant $C$ is related to the critical stress intensity factor, which is, in turn, related to the critical strain energy release rate. For discrete systems, such as a fiber network, however, there is no stress singularity, and "cracks" (i.e., damage clusters) are not necessarily linear or oriented perpendicular to the loading direction. They are also not necessarily contiguous or node sharing as a result of pinning or depinning of the damage growth in the disordered structure. However, in the case of ordered structures in the quasibrittle and brittle range ($\rho \geqslant 5$), we have observed a cracklike damage cluster that triggers the avalanche failure of the entire system [Figs. 8(a) and 8(b)]. Therefore, we have determined the critical crack length as the number of damaged elements in the critical cluster and plotted the crack length against the brittleness parameter of the fiber $\rho_f$ (Fig. 7). With increasing $\rho_f$, the average critical length sharply decreased, and only a very small number of damages were required to trigger the avalanche. We can also see that with decreasing brittleness the error-bar size for critical crack length increases, suggesting that so-called crack is becoming more difficult to define.

In the case of disordered structures, the situation is very different. Figure 8 shows two snapshots of damage clusters taken just before the avalanche failure of the network for each SD value. The value of $\rho_f$ is set to 10, corresponding to a quasibrittle case. For the original ordered structure (SD = 0), we can clearly see a cracklike damage cluster, which eventually triggers the avalanche failure. However, as soon as we introduce structural disorders (SD = 0.1 and 0.28), such crack shape disappears, and the dominant damage clusters become less defined entities. In other words, for the ordered structure, the dominant clusters look like cracks, whereas for

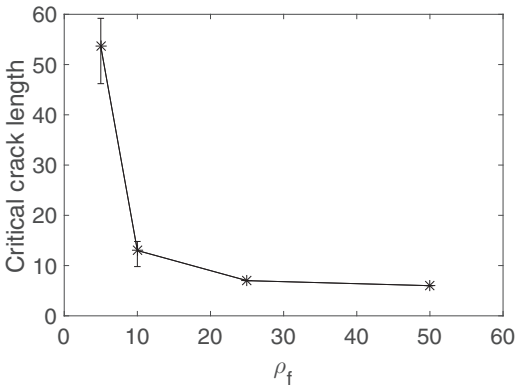


FIG. 7. Number of continuous damaged elements required for avalanche failure (critical crack length) vs brittleness parameter, $\rho_f$.

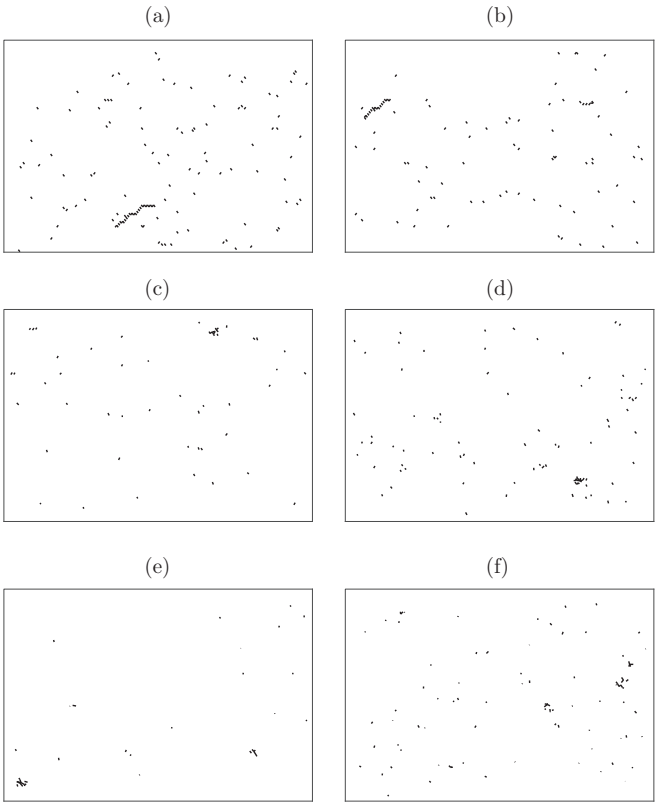


FIG. 8. Snapshots of damages just before avalanche failure. (a) and (b) Standard deviation SD = 0; (c) and (d) SD = 0.1; and (e) and (f) SD = 0.28.

the disordered structures, they are more like "voids," as broken fibers tend to share the same node. It should be noted that, for these simulations, although we can see extensive fiber breakages just before the avalanche, the system is still rigid in terms of "$p$ value" (the probability of finding intact fibers in the network), $p > 0.99$, far from the rigidity transition point ($p_c \simeq 0.6602$) [48].

## V. DISCUSSION

The central question of this study is why time-dependent failure of many materials often shows enormous variability, with a COV of more than 100% (or $\beta_s \leqslant 1$). The Weibull shape parameter of lifetime distribution, $\beta_s$, is proportional to the same parameter of the fiber, $\beta_f$. The proportional constant varies with the brittleness of the fiber, $\rho_f$, but maintains values greater than unity for ordered networks. For disordered networks, however, the values can be less than unity, depending on the degree of the structural disorder. Figure 9 shows a summary of the effects of different types of disorder on the Weibull shape parameter of the network, $\beta_s$. The data for the strength and stiffness disorders are taken from our previous study [40]. [The strength disorder was created by varying the characteristic strength $T_c$ in Eq. (8) according to a continuous uniform distribution function, and the stiffness disorder was generated by varying the cross-sectional area of fiber (truss) drawn from the uniform distribution.] Interestingly, the strength disorder has a rather modest impact on $\beta_s$, whereas

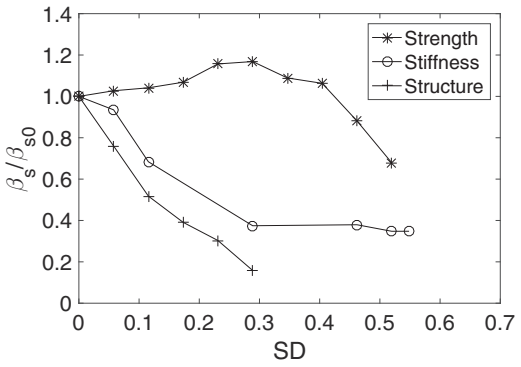


FIG. 9. Effects of different types of disorders on $\beta_s$. SD is the standard deviation.

the stiffness and structural disorders have a strong negative impact on the parameter. A natural speculation from this result is that the system variability may be more influenced by stress distributions within the structure, rather than "threshold" strength distributions.

WLS-like scaling of the lifetime distribution emerges slowly as the network size increases. We have obtained an explicit form of the characteristic distribution that is not a Weibull distribution but instead has a double-exponential form (DLB-type distribution). The implication of this result with respect to lifetime uncertainty is important. Suppose the Weibull shape parameter measured for a finite-size specimen is less than unity. This means an infinite rise of probability density for short lifetimes according to the Weibull distribution. However, Eq. (20) suggests that, as the system size increases and enters the WLS range, the probability density does not grow to infinity but approaches zero instead. This is a huge difference from the estimate based on the Weibull distribution. The situation is, however, different for the material design based on quasistatic strength where Weibull estimate is merely a "conservative" estimate. In other words, the implication of non-Weibull behavior is far more significant for TSF than for QSF.

A nontrivial result from this study is that $\rho_f = \rho_s$: load scaling on the fiber level is preserved even at the network level. The brittleness of the fiber network is controlled by the brittleness of the fiber. This property is unique to the power-law form of damage growth, and it was first recognized by Phoenix and Tierney through their fiber-bundle model [26]. We have extended it to a general fiber network case and validated it via numerical experiments. This relation is restricted to the case in which the system exhibits material and geometrical linearity (i.e., small elastic deformations). Of course, the deviation occurs when a matrix material with a high creep exponent is introduced into fiber-reinforced composites [52]. Nevertheless, the relation indicates the fundamental impact of fiber brittleness on the brittleness of a fiber network.

## VI. SUMMARY AND CONCLUSIONS

We have investigated the reason for large uncertainty of lifetime and its asymptotic distribution with system size by numerical simulations of creep failure with a triangular-lattice, spring network model.

Coleman's and Christensen's models explain why static strength distribution is much smaller than that of creep lifetime, at least, on a phenomenological level. For static strength, monotonic loading, stress sensitivity of damage creation (i.e., $\rho$), and stress enhancement at damage sites, all together prevent damage evolution from an extensive excursion in the disordered field, thus reducing much of the uncertainty [Eq. (1)]. However, for creep failure, the underlying stochastic failure process (thermal fluctuations) has ample opportunity of competing and interacting with different types of disorders in the network. Comparing the three types of disorders: threshold strength, stiffness (stress), and network geometry, we have found the largest impact of the geometrical disorder on uncertainty of lifetime. Particularly, increasing disorder in the structure alters critical damage clusters from one (or a few) linear crack(s) to more numbers of irregular-shaped objects. This lack of a predominant damage cluster (crack) at the time of cascading failure obviously contributes to the increased uncertainty of lifetime.

We have found that, with increasing system size, the creep lifetime distribution asymptotically approaches the DLB-type distribution, which was earlier shown for static strength by using a random fuse model [34,38] and fiber-bundle models [31,35]. The presence of the same form of distribution for creep lifetime and in the 2D system is intriguing. One possible reason for the emergence of the DLB-type distribution is that the problem of lifetime statistics of fiber may be transformed into an equivalent probability model of fiber failure through the damage parameter [Eq. (3.15) in [26]]. In other words, one can recast the lifetime statistics problem to a usual strength statistics problem. Another reason may come from the damage size distribution. It was indicated that the physical origin of the DLB-type distribution is related to the exponential tail of damage cluster size distribution [35]. Therefore, if the exponential tail of the damage cluster size distribution is shown to be universal (e.g., [38,53]), then the emergence of the DLB-type distribution is expected even for lifetime.

## ACKNOWLEDGMENTS

The authors acknowledge the financial support provided by the KK-Foundation in Sweden and valuable discussions and experimental support received from SCA R&D and BillerudKorsnäs. The authors would also like to thank the anonymous reviewer of their earlier paper for suggesting the investigation of randomly distorted networks.

[1] S. L. Phoenix, Int. J. Fract. **14**, 327 (1978).
[2] H. D. Wagner, P. Schwartz, and S. L. Phoenix, J. Mater. Sci. **21**, 1868 (1986).
[3] H. F. Wu, S. L. Phoenix, and P. Schwartz, J. Mater. Sci. **23**, 1851 (1988).
[4] S. L. Phoenix, P. Schwartz, and H. H. Robinson IV, Compos. Sci. Technol. **32**, 81 (1988).
[5] D. Farquhar, F. Mutrelle, S. L. Phoenix, and R. L. Smith, J. Mater. Sci. **24**, 2151 (1989).
[6] H. Otani, S. Phoenix, and P. Petrina, J. Mater. Sci. **26**, 1955 (1991).
[7] A. Mattsson and T. Uesaka, in *Advances in Pulp and Paper Research, Transactions of the 15th Fundamental Research Symposium*, Vol. 1, edited by S. I'Anson (The Pulp and Paper Fundamental Research Society, Cambridge, UK, 2013), pp. 711–734.
[8] J.-L. Le and Z. P. Bažant, Math. Mech. Solids **19**, 56 (2014).
[9] B. D. Coleman, J. Appl. Phys. **29**, 968 (1958).
[10] B. D. Coleman, J. Appl. Phys. **28**, 1058 (1957).
[11] B. D. Coleman, J. Polym. Sci. **20**, 447 (1956).
[12] R. M. Christensen, Mech. Time-Depend. Mater. **8**, 1 (2004).
[13] R. Christensen and Y. Miyano, Int. J. Fract. **137**, 77 (2006).
[14] M. Alava, P. K. V. V. Nukala, and S. Zapperi, Adv. Phys. **55**, 349 (2006).
[15] W. A. Curtin and H. Scher, Phys. Rev. B **55**, 12038 (1997).
[16] W. I. Newman and S. L. Phoenix, Phys. Rev. E **63**, 021507 (2001).
[17] W. Curtin, Adv. Appl. Mech. **36**, 163 (1999).
[18] Z. P. Bažant and Y. Xi, J. Eng. Mech. **117**, 2623 (1991).
[19] Z. P. Bažant and D. Novák, J. Engg. Mech. **126**, 175 (2000).
[20] Z. Bažnt, Proc. Natl. Acad. Sci. U. S. A. **101**, 13400 (2004).
[21] D. T. Hristopulos and T. Uesaka, Phys. Rev. B **70**, 064108 (2004).
[22] H. Daniels, Proc. R. Soc. London, Ser. A **183**, 405 (1945).
[23] D. G. Harlow and S. L. Phoenix, J. Compos. Mater. **12**, 195 (1978).
[24] D. G. Harlow and S. L. Phoenix, Int. J. Fract. **15**, 321 (1979).
[25] W. Curtin, Compos. Sci. Technol. **60**, 543 (2000).
[26] S. L. Phoenix and L. Tierney, Eng. Fract. Mech. **18**, 193 (1983).
[27] W. I. Newman and A. M. Gabrielov, Int. J. Fract. **50**, 1 (1991).
[28] S. L. Phoenix and I. J. Beyerlein, Phys. Rev. E **62**, 1622 (2000).
[29] S. Pradhan, A. Hansen, and B. K. Chakrabarti, Rev. Mod. Phys. **82**, 499 (2010).
[30] A. Hansen, P. C. Hemmer, and S. Pradhan, *The Fiber Bundle Model: Modeling Failure in Materials* (Wiley, New York, 2015).
[31] B. Q. Wu and P. L. Leath, Phys. Rev. B **59**, 4002 (1999).
[32] S. Eggwertz and N. C. Lind, *Probabilistic Methods in the Mechanics of Solids and Structures: Symposium Stockholm, Sweden, 1984* (Springer Science & Business Media, Stockholm, 2012).
[33] R. A. Fisher and L. H. C. Tippett, in *Mathematical Proceedings of the Cambridge Philosophical Society* (Cambridge University Press, Cambridge, UK, 1928), Vol. 24, pp. 180–190.
[34] P. M. Duxbury, P. L. Leath, and P. D. Beale, Phys. Rev. B **36**, 367 (1987).
[35] P. M. Duxbury, S. Kim, and P. L. Leath, Mater. Sci. Eng. A **176**, 25 (1994).
[36] P. M. Duxbury and P. L. Leath, Phys. Rev. B **49**, 12676 (1994).
[37] Z. Bertalan, A. Shekhawat, J. P. Sethna, and S. Zapperi, Phys. Rev. Appl. **2**, 034008 (2014).
[38] C. Manzato, A. Shekhawat, P. K. V. V. Nukala, M. J. Alava, J. P. Sethna, and S. Zapperi, Phys. Rev. Lett. **108**, 065504 (2012).

[39] W. A. Curtin and H. Scher, Phys. Rev. B **45**, 2620 (1992).
[40] A. Mattsson and T. Uesaka, Phys. Rev. E **92**, 042158 (2015).
[41] W. A. Curtin and H. Scher, J. Mater. Res. **5**, 535 (1990).
[42] M. Vujosevic and D. Krajcinovic, Int. J. Solids Struct. **34**, 1105 (1997).
[43] A. Kulachenko and T. Uesaka, Mech. Mater. **51**, 1 (2012).
[44] J. C. Maxwell, Philos. Mag. **27**, 294 (1864).
[45] J. C. Phillips, J. Non-Cryst. Solids **34**, 153 (1979).
[46] M. Thorpe, J. Non-Cryst. Solids **57**, 355 (1983).
[47] M. M. Driscoll, B. G.-g. Chen, T. H. Beuman, S. Ulrich, S. R. Nagel, and V. Vitelli, Proc. Natl. Acad. Sci. USA **113**, 10813 (2016).
[48] L. Zhang, D. Rocklin, L. M. Sander, and X. Mao, arXiv:1612.08911.
[49] J. Koivisto, M. Ovaska, A. Miksic, L. Laurson, and M. J. Alava, Phys. Rev. E **94**, 023002 (2016).
[50] W. Newman, A. Gabrielov, T. Durand, S. Phoenix, and D. Turcotte, Physica D **77**, 200 (1994).
[51] H. Rahami, Truss analysis (2007), http://www.mathworks.com/matlabcentral/fileexchange/14313-truss-analysis/ (accessed May 28, 2015).
[52] S. Mahesh and S. Phoenix, Int. J. Fract. **127**, 303 (2004).
[53] C. Manzato, M. J. Alava, and S. Zapperi, Phys. Rev. E **90**, 012408 (2014).